Geoelectrical and hydrogeochemical assessment of groundwater sources of Nkpor metropolis Southeastern Nigeria

Udegbunam Innocent Ejike*, Okoyeh E I, Anaekwe Michael U, Okpara Augustine O

Udegbunam IE, Okoyeh EI, Anaekwe Michael U, et al. Geoelectrical and hydrogeochemical assessment of groundwater sources of Nkpor metropol -is Southeastern Nigeria. J Environ Geol. 2021;5(2):1-12.

ABSTRACT

Electrical resistivity and hydrogeochemical investigations have been carried out to determine the groundwater potentials and aquifer parameters in Nkpor Southeastern Nigeria. Vertical Electrical Sounding Survey (VES) and hydrogeochemical studies were employed in this research. Twelve Vertical Electrical Sounding (VES) curves were obtained across the area using the Schlumberger configuration. The result of the VES survey shows that the subsurface layers ranged from 3 to 6. The depth to water ranges from 25 m to 114 m. Aquifer thicknesses range between 20 m to 60 m. The hydraulic conductivity (K) ranged from 0.25 m/day to 3.027 m/day while the transmissivity (T) ranged from 8.2 m^2/day to 166.49 m^2/day. The hydrochemical analysis of groundwater samples collected from twenty sample points within the study area reveals that all ionic components are within the acceptable limits, with the exception of heavy metals like Fe and Cd. The pH values reveal that they are acidic waters. The study revealed that the mean value of Fe (0.832000 ± 1.0626228 ppm) and Cd (0.043750 ± 0.0181713 ppm) exceeded the permissible limit for NSDWQ water quality standard. Water Quality Index (WQI) revealed that 80% of the samples are of good quality for drinking purpose. The Heavy Metal Pollution Index (HPI) and degree of contamination (Cd) also revealed that most of the samples are of low level of pollution whereas Heavy Metal Evaluation Index (HEI) revealed that only 5% of the samples are of low level of pollution. The Sodium Adsorption Ratio (SAR) model revealed that 40% (8 samples) of the samples were excellent for irrigation, 45% (9 samples) are of good quality, 10% (2 samples) were fair while 5% (1 sample) is of poor quality for irrigation. However, Kelly's Ratio (KR) model shows that 100% of the samples are unsuitable for irrigation purposes while the Magnesium Adsorption Ratio (MAR) revealed that 30% (6 samples) of the samples are acceptable and 70% (14 samples) not acceptable. Moreover, the Sodium Percentage (Na%) model revealed that only 5% (1 sample) of the samples is good for irrigation, 55% (11 samples) are permissible while 40% (8 samples) are doubtful. The Permeability Index (PI) revealed that 70% of the samples are of excellent quality while 30% are of good quality for irrigation purposes. In all the hydrochemical facies classification applied, they confirmed that the groundwater in the study area is dominantly sodium chloride waters. This research is expected to help water resource planners taking adaptive measures for groundwater quality monitoring in the study area.

Key Words: *Electrical resistivity; hydrogeochemical; groundwater potentials; Vertical Electrical Sounding Survey.*

INTRODUCTION

Water is generally accepted as the principal component of life. Its availability in the right quality and quantity is integral to supporting socio-economic development and vital ecosystems which depend upon it [1,2]. Water is known to occur naturally in the surface of the earth (surface water) and beneath the earth surface. Surface waters has been the major source of drinkable water since the beginning of mankind or since creation and because of population growth and economic development, surface water in many parts of the world are pushed to their natural limits [1].

Groundwater is that water contained in the voids of the geologic materials that comprise the crust of the earth and exists at a pressure greater than or equal to atmospheric pressure [3]. Natural and anthropogenic activities are threatening water availability and its suitability for multiple uses [4]. Surface water has suffered most from both anthropogenic and climate change [5]. Hence, the search for groundwater which is strategically valuable because of its high quality and availability as it represents about 97% of the planet's fresh water [6]. Since groundwater is normally hidden from view, there is difficulty in visualizing the occurrence and movement of groundwater by water borehole drillers. As a consequence, this complexity adversely affects the ability to understand and to deal effectively with groundwater related problems. To remedy this situation, a precise and detailed knowledge of the subsurface geology is necessary to elucidate the behaviour of groundwater aquifer in the area and a geophysical survey is a useful approach to this.

Geophysical methods are methods that use the physical properties of earth materials to interpret subsurface structure. The electrical resistivity value of geological formations depends on the lithological properties (density, porosity, pore size and shape), and water content and its quality and temperature [7]. Geophysical methods are relevant in hydrological applications and in determining aquifer hydraulic properties [3,8,9]. DC-resistivity measurements can contribute significantly to enhance the correctness of the groundwater model by delineating aquiferous zones, using the established relationship between geoelectrical and hydro geological parameters [10]. Vertical Electrical Sounding (VES) survey has proved to be an effective and a reliable geophysical survey technique in locating viable aquifers for continuous and regular water supply [11]. Electrical resistivity methods have been extensively used for groundwater investigation by many workers [12] and it is considered to be the most suitable method for groundwater investigation in most geological Terrains due to its simplicity and low cost.

Research in groundwater geophysics reveals that a correlation exists between the hydraulic parameters and geoelectric properties of an aquifer and this can be used as a possible solution to cut the cost of wildcat drilling, pumping test etc. [13-16]. Relationships between aquifer characteristics and geoelectrical parameters have been studied and reviewed by many authors [15-32]. Interpretation of true thickness and subsurface layers of aquiferous area measured from resistivity measurements have been made possible through the use of computer modelled interpretation procedure [25,33,34]. Both direct and inverse relations between aquifer resistivity and hydraulic conductivity are reported [15,17,22,35].

Vertical Resistivity Soundings (VES) have been used in this study to assess its possible relationship with hydraulic conductivity and transmissivity estimates in the study area following the ideas explored by Niwas et al. [19] and Mazac O et al. [22]. Hydro chemical analysis of the study area has also been carried out to assess the quality of the groundwater with a view to determine the portability.

DESCRIPTION OF THE STUDY AREA

Location

The study area covers an area extent of approximately 145 square kilometers and situated within latitudes 6° 7′ 0″ N to 6° 12′ 30″ N, and longitudes 6° 46′

Nnamdi Azikiwe University, Awka

Correspondence: Udegbunam IE. Nnamdi Azikiwe University, Awka, Tel: 07036332683; E-mail: innoejike@gmail.com

Received: January 26, 2021, Accepted: February 25, 2021, Published: March 03,2021

0" E to 6° 54' 30" E. The study area is characterized by an extensive flood plain that covers the entire Iyowa-Odekpe community in the southwestern part that harbours the industrial layout with an average elevation of about 26 m while in the northeast elevation ranges from 34 m to 159 m above sea level. Nkpor, Onitsha, Obosi, Ogidi, Odekpe and Atani are the most industrialized, populated, and commercial centers of the study area. The study area is accessible through Enugu-Onitsha express way and Nkpor old road and other minor roads. Figure 1 shown below is the accessibility map of the study area.

Climate

The study area falls within the tropical environment which is characterized by two seasons; rainy season and dry season. Rainy season starts around March to October, during which the area experiences high precipitation. These seasonal climatic conditions are caused by the north-south fluctuations of a zone of discontinuity between the dry continental air mass and the humid maritime Atlantic air mass [36]. The rainy season follows the advancing atlantics maritime air which is accompanied by high humidity and intense rain. Peak rainfalls occur during the months of June to September. There is characteristic "August break" lasting about 2 weeks. This occurs during the month of August but may extend to early September. (Tables 1-4) shows the ten years mean annual meteorological data obtained from the Department of Hydro-Meteorology, Ministry of Tertiary Education, Science and Technology Awka Anambra State. Figure 2 shows the mean annual seasonal variation in precipitation and their maximum and minimum temperature for the ten years (2009-2018) period. The rainfall data covering the period 2009-2018 gave an annual average rainfall of 2042.65 mm. The figure indicates that the combined average precipitation of 2042.65 mm could be attributed to excessive rainfall in months of July and September. The months of July and September are commonly the wettest months in the study area. The mean annual maximum temperature is about 33°C and the mean minimum temperature is about 23°C. The mean annual temperature is about 28°C. From (Figure 2), it is observed that maximum temperatures are experienced in the December-March period and minimum temperatures in the June-September period. The pattern of the climate is reflected more in the rainfall pattern. Figure 3 shows the mean annual seasonal variation in precipitation and the relative humidity for the period often years (2009-2018). The relative humidity is generally high throughout the year, between 60% and 80%. The highest figures are experienced during the wet season and the lowest during the dry season. The mean annual relative humidity is 81%.

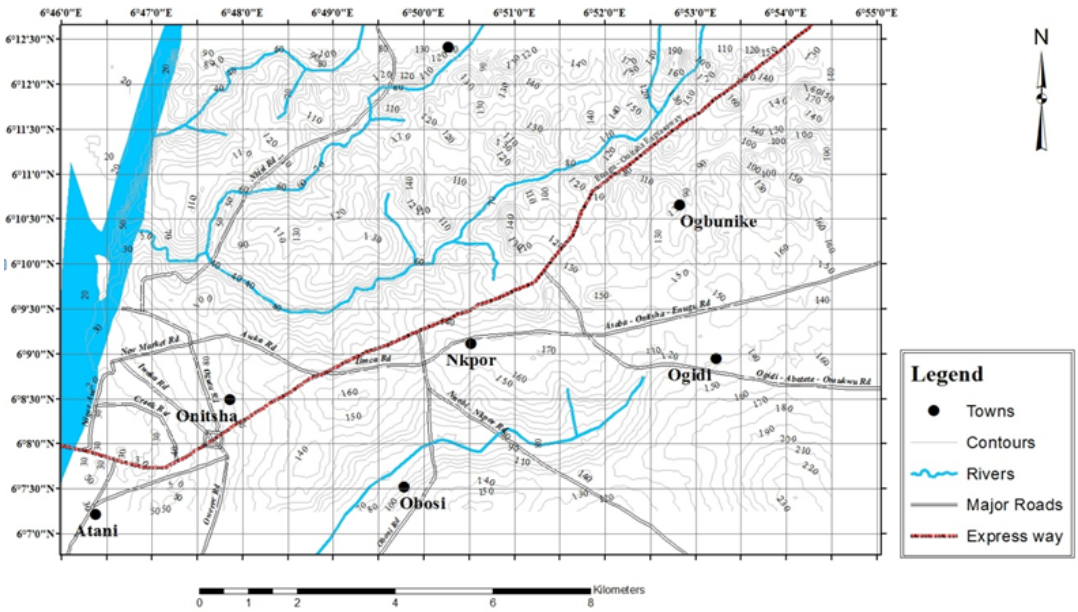

Figure 1) Map of the study area.

TABLE 1
Rainfall data

Months	2009	2010	2011	2012	2013	2014	2015	2016	2017	2018	Total	Average
Jan.	60.4	4.3	0	38	37.1	37.6	0	0	3.6	0	180.97	18.1
Feb.	5.6	45.1	19.8	72	0	16.4	66.8	0	6.1	23.1	254.88	25.5
March	30.4	44	71.7	22	60.4	134	92.8	84.1	66.7	38.5	644.8	64.5
April	118.8	181.9	93.4	159.5	95.7	162	84.4	132	307.9	229.2	1564.95	156.5
May	208.2	151.2	261.4	237.1	270	209	224	198.5	180.7	171.7	2111.7	211.2
June	182.9	295.2	229.3	332.3	291.4	178	223.4	326.7	401.3	292.7	2753.4	275.3
July	402.6	178.7	243.5	358.8	267.2	237	379.2	323.6	416	684.8	3491.1	349.1
Aug.	244.7	303.8	285.3	377.1	226.1	253	167.2	314.5	323.2	405.2	2900.2	290
Sept.	222.6	378.7	279.6	280.1	281	330	481	274.4	484.2	446.4	3457.7	345.8
Oct.	343.1	218.4	355.6	233.6	212.3	174	246.1	197.4	182.7	233.1	2396.2	239.6
Nov.	96.3	81.4	25.8	89.3	4.7	135	60	22.7	37.6	93.4	646.6	64.7
Dec.	0	0	0	0	16.1	5.4	2.4	0	0	0	24	2.4
												2042.7

TABLE 2
Relative humidity data.

Months	2009	2010	2011	2012	2013	2014	2015	2016	2017	2018	Total	Average
Jan.	76	72.7	59.8	72.7	73.2	73.7	58.6	53.6	70.6	65.3	676.2	67.6
Feb.	81	76.7	77.8	80.6	75.4	80.3	79.8	70.4	69.6	77.3	768.9	76.9
March	77	76.4	76.9	77.8	78.7	81.7	80.3	82.3	76.9	79	787	78.7
April	81	79.4	80.5	80.2	80.3	81.5	81	81.2	79.7	83.4	808.2	80.8
May	81.8	83	84	81.9	83.5	86.1	81.8	82.8	83.4	74.9	823.2	82.3
June	85.2	86.3	84.6	83.5	86.1	86.5	85.9	86.1	85.3	84	853.5	85.4
July	88.8	85.6	88.1	87.5	89.8	87.6	88.5	87.4	87	88.2	878.5	87.9
Aug.	87.5	86.7	90.5	88.6	90.1	90	90.2	89.1	87.8	88.4	888.9	88.9
Sept.	86	86.9	88	86.1	89.4	89.4	88	88.6	88.4	87.6	878.4	87.8
Oct.	83.6	84.2	84.5	86.7	85.5	86.5	86	85.8	86.3	85.7	854.8	85.5
Nov.	78	82.3	80	83	81.8	83.6	82.7	80.3	82.2	82.1	816	81.6
Dec.	77.8	73.5	68.5	73.3	74.6	70	61	72.2	72.4	59.9	703.2	70.3
												973.7

TABLE 3
Maximum temperature data

Months	2009	2010	2011	2012	2013	2014	2015	2016	2017	2018	Total	Average
Jan.	33.8	34.6	33.8	33.3	34.7	34.8	34.1	35.1	35.2	35.2	344.6	34.5
Feb.	34.2	35.5	33.5	33.2	34.5	34.7	35.2	36.3	35.7	35.6	348.4	34.8
March	35.6	35.5	34.1	34.5	35.1	34.3	34.7	35.3	36	35.4	350.5	35.1
April	33.9	34.1	33.1	33.6	34.2	34.1	33.5	34.6	34.5	33.7	339.3	33.9
May	33.2	33	32.4	32.1	32.6	32.5	34	34.4	33.3	33	330.5	33.1
June	31.8	30.6	30	30.9	31.2	31.3	31.1	31.7	32.6	32	313.2	31.3
July	30.5	30.3	29.8	29.8	30.4	30.1	31.4	30.5	31.1	29.9	303.8	30.4
Aug.	30	30.2	29.2	29.2	29.5	29.3	30	29.9	30.7	29.5	297.5	29.8
Sept.	29.3	30.8	29.4	30.3	29.7	29.8	30.9	31.1	30.5	31	302.8	30.3
Oct.	30.6	31.8	31.6	31.1	31.5	31.8	32	32.6	31.9	31.5	316.4	31.6
Nov.	33.1	31.5	32.9	32.2	33.4	32.6	33.6	33.5	33.1	33	328.9	32.9
Dec.	35	33.7	34.1	33.6	33.7	33.7	34.6	34.8	33.9	34.6	341.7	34.2
												391.9

Table 4
Minimum temperature data.

Months	2009	2010	2011	2012	2013	2014	2015	2016	2017	2018	Total	Average
Jan.	22.4	23.3	19.5	20.4	21.9	21.6	19.9	20.3	22.9	20.4	212.6	21.3
Feb.	24.9	25	23.9	23.7	23.6	23.7	23.3	23.2	24	22.9	238.2	23.8
March	25.3	25.1	24.3	24.5	24.1	23.7	24	24.5	25	24.2	244.7	24.5
April	24.2	24.7	23.9	23.3	23.9	23.7	23.4	24.3	24.5	22.8	238.7	23.9
May	23.3	24.1	23.4	22.2	23.2	23.5	23.3	26.6	24	22.5	236.1	23.6
June	23.1	24	23.1	22.2	22.3	23.5	23.4	23.7	23.3	22.9	231.5	23.2
July	23.1	23.4	22.2	21.9	22.4	23.4	23.3	23.3	23.4	22.1	228.5	22.9
Aug.	23.3	23.3	23	21.7	22.6	23	23.4	23.4	23.3	23	229.6	23
Sept.	23.1	22.7	23	22.5	22.6	23.1	23.1	23.2	23	22.2	228.5	22.9
Oct.	22.5	23	22.6	22.2	22.9	23.1	23.7	23.4	23.3	22.5	229.2	23
Nov.	22.6	23.8	23	22.9	23.4	23.5	24.3	23.6	23.8	23.2	234.1	23.4
Dec.	22.1	21.9	20.6	21	22	21.6	20.5	23.1	22.5	20.5	215.8	21.6
												277.1

GEOLOGY AND HYDROGEOLOGY

The study area is underlain by the Ameki Group and at the western part of the area is bounded by the River Niger with the edge of the River housing the Alluvium deposits. The Ameki Group is Eocene in age and its lateral facies equivalent is the Nanka Sand, Ameki Formation and the Nsugbe Sandstone. The Ameki Formation consists of a series of highly fossilliferous grayish-green sandy clay with calcareous concretions and white clayey sandstone [37]. It compresses two lithological groups. The lower groups are fine to coarse grained sandstone with intercalation of calcareous shale and thin shaly limestone while the upper group is coarse grained cross bedded sandstone with bands of fine grey-green sands and sandy clay [38]. Refer to the Ameki Formation to have between 1200 ft to 1500 ft with regressive facies, shallow marine environment [39]. Its lateral equivalent is Nanka sand. The study area is drained by three major rivers:

- Anambra River, located at the northern part of the study area, flowing westward into the River Niger
- The Nkisi River, located at the central part of the study area, flowing westward into the River Niger
- The Idemili River, located at the southern part of the study area, flows westward into the Niger River

In the study area, the groundwater resources can be accessed through wells and boreholes. The wells are dug in regions of high hydraulic heads (where the aquifer is shallow) and the boreholes are drilled where the aquifer is moderately deep. Groundwater resources always flow from region of high hydraulic head to region of low hydraulic head. Geologic map of the study area is shown in figure 4 below.

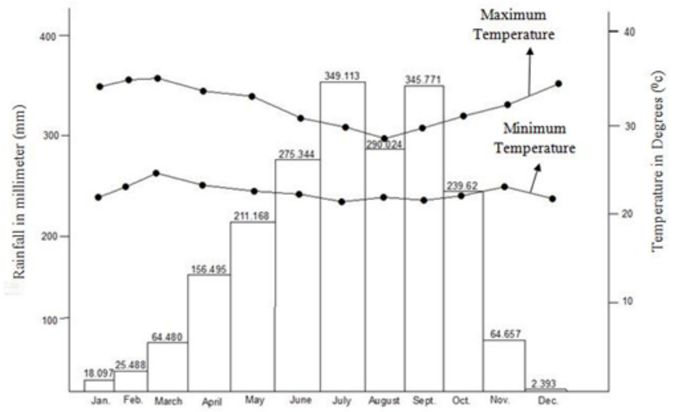

Figure 2) Ten years (2009-2018) average rainfall and temperature.

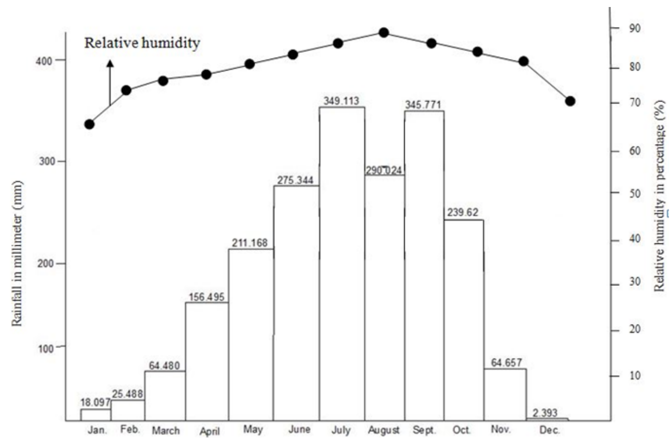

Figure 3) Ten years (2009-2018) average rainfall and relative humidity.

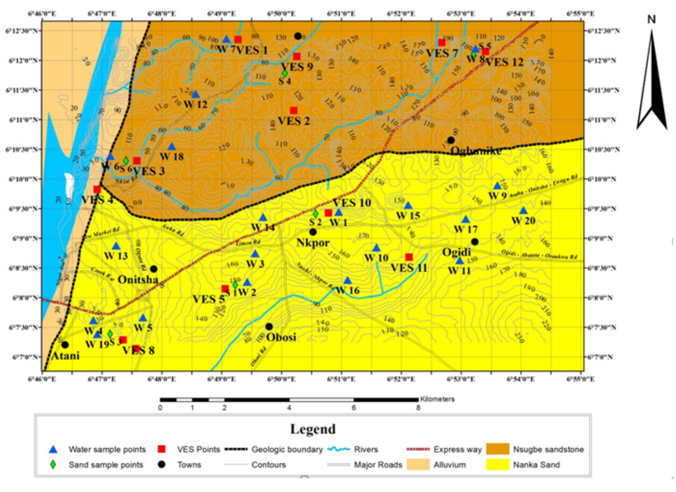

Figure 4) Geologic map of the study area showing sample locations.

MATERIALS AND METHODS

Vertical electrical sounding survey and hydrogeochemical studies were employed in this research.

VERTICAL ELECTRICAL SOUNDING SURVEY (VES)

Twelve [36] vertical electrical soundings (VES) were carried out in the study area using OHMEGA SAS1000 Terrameter with its accessories. The Schlumberger electrode array was employed for each VES profile with half current (AB/2) electrode separation of 150 m and half potential (MN/2) electrode separation of 15 m. This procedure is known to generate reliable subsurface stratigraphic contrasts. This technique uses two pairs of electrodes technically referred to as the current and potential electrodes connected to a resistivity meter. The geoelectric soundings were taken at the site of existing boreholes for the purpose of comparison in order to establish the interrelationship between the geoelectric sections and subsurface geo-electrical layer.

The apparent resistivity was computed using equation (1);

$$\rho_a = \pi . \left(\frac{\left(\frac{AB}{2}\right)^2 - \left(\frac{MN}{2}\right)^2}{MN} \right) . \frac{\Delta V}{I} \quad (1)$$

Where ρ_a is the apparent resistivity, π is $\frac{22}{7}$

$$G = \pi . \left(\frac{\left(\frac{AB}{2}\right)^2 - \left(\frac{MN}{2}\right)^2}{MN} \right) = \text{G Geometric factor and } \frac{\Delta V}{I} = R\,(\text{Resistance})$$

The apparent resistivity values obtained from equation (1) were plotted on bi-logarithmic graph against the half current electrode separation spacing and the curves generated were smoothened to remove the effects of lateral inhomogeneities and other forms of noisy signatures [40,41]. From these plots, qualitative deductions, such as the resistivity of the first or top layer, the depth of each layer, and the curve signatures or types were made. The ZOND computer software was employed for carrying out the iteration and inversion processes.

The hydraulic conductivity was estimated using the equation as given by 13:

$$K = 386.40 R_{rw}^{-0.93283} \quad (2)$$

Where, *K* is the hydraulic conductivity and R_{rw} is the aquifer resistivity.

The transmissivity values were calculated using [42]:

$$T = Kh \quad (3)$$

Where, T is transmissivity, K is hydraulic conductivity and h is aquifer thickness. This provides a general idea of the water producing capabilities of aquifer from surficial electrical methods.

The total longitudinal conductance (S_T) of the overburden unit at each vertical electrical sounding station was obtained from the mathematical relation [43]:

$$S_T = \sum_{i=1}^{n} \frac{hi}{\rho i} \quad (4)$$

Where S_T=total longitudinal conductance of the overburden, ρi=layer resistivity, hi=layer thickness, and n=number of layers and were used to characterize the aquifer protective capacity of the area.

The longitudinal conductance (S) was calculated thus:

$$S = \frac{h}{\rho} \quad (5)$$

Where, h is layer thickness of the aquifer and ρ is layer resistivity of the aquifer.

HYDROCHEMICAL INVESTIGATION

A systematic sampling technique was utilized to sample groundwater from the study area. A total of twenty [20] groundwater samples were collected. Direct contact with the well owners was made on arrival before sample collection. Global Positioning System (GPS) was used to record the coordinate of each sample location. The groundwater was allowed to flow for 5 minutes before collection. The samples were collected with a 2 litre polyethylene can washed and rinsed three times with the sample to be collected. The samples collected were sealed off immediately and preserved with ice before taking them to laboratory where they were analysed within 24 hours using Varian AA 240 Atomic Absorption Spectrophotometer (AAS), according to the specification of American Public Health association [44].

RESULTS AND DISCUSSIONS

Vertical electrical soundings

The following procedures were employed in interpreting the results:

- Interpretation of the vertical electrical sounding curves using the ZOND Software
- Generation of geoelectric sections and its correlation with lithologic log from ongoing boreholes
- Determination of Aquifer thickness and the depth to water table from the sounding curves

Interpretation of the vertical electrical sounding curves

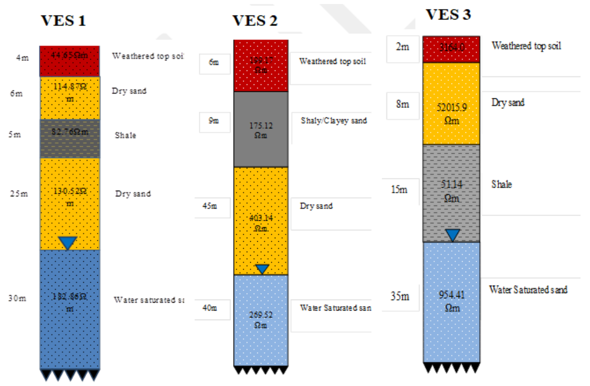

Figure 5a) Geo-electric log of VES 1-3.

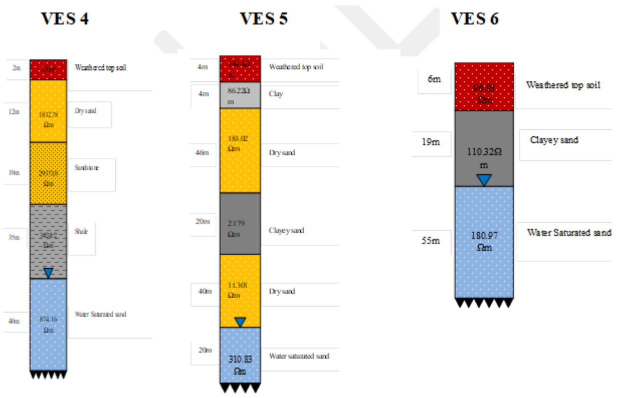

Figure 5b) Geo-electric log of VES 4-6.

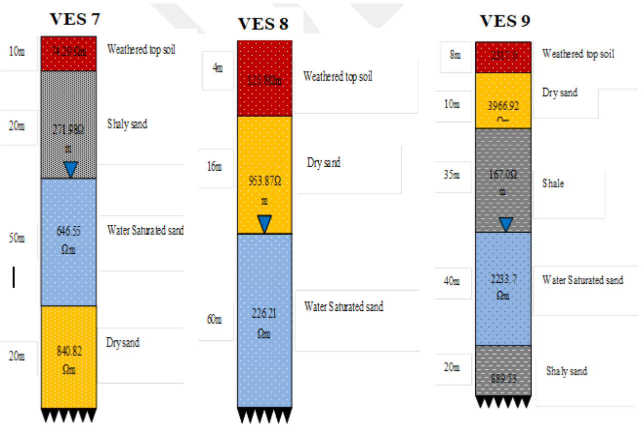

Figure 5c) Geo-electric log of VES 7-9.

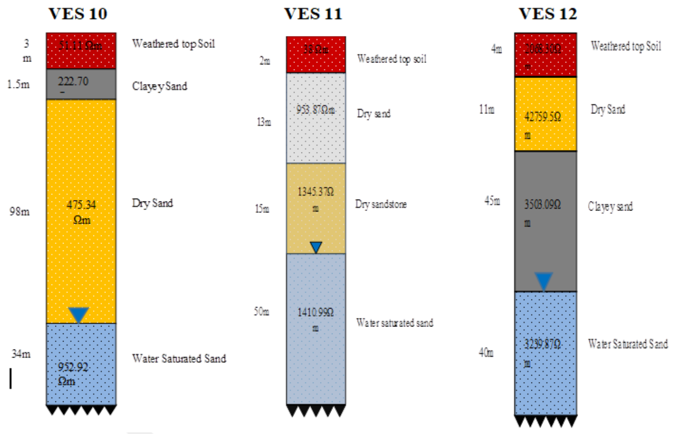

Figure 5d) Geo-electric log of VES 10-12.

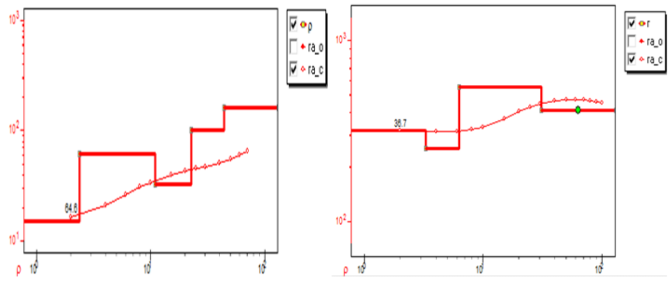

Figure 6a) Curve for VES 1 and 2.

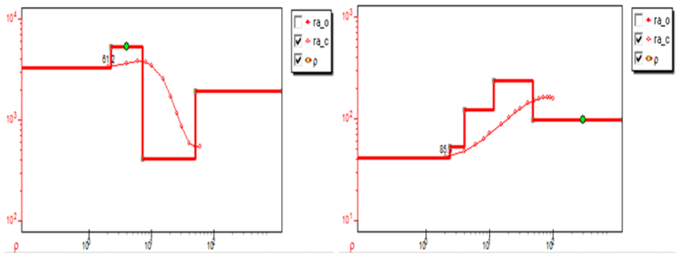

Figure 6b) Curve for VES 3 and 4.

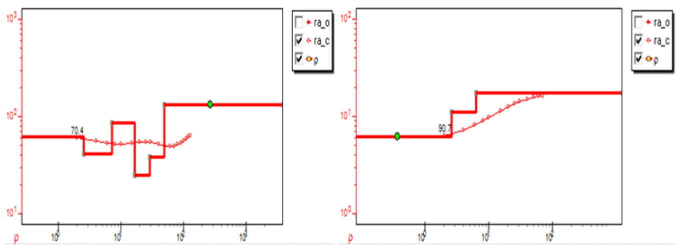

Figure 6c) Curve for VES 5 and 6.

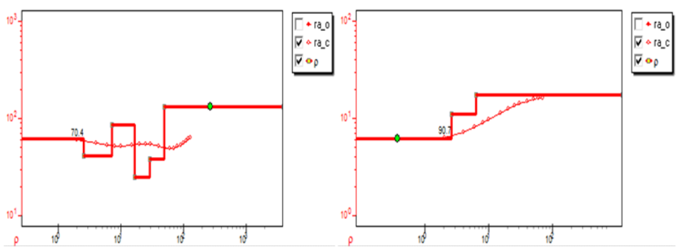

Figure 6d) Curve for VES 7 and 8.

CORRELATION OF GEO-ELECTRIC LOG AND LITHOLOGY LOG

Borehole logs were obtained from ongoing boreholes within the study area. The logs were correlated with geoelectric section obtained from VES. Litho-log data was obtained from borehole data from the study area. Figure 7 shows the correlation and subsequent interpretation of geo-electric logs and borehole log of the study area.

DEPTH TO WATER AND AQUIFER THICKNESS

The depths to groundwater (Figure 8), across the study area, were determined from the sounding results. The deduction shows that the depth to groundwater is generally shallow towards the western part of study area. It ranges from 20m to 114m with aquifer thicknesses ranging from 20 m to 60 m (Figure 9).

Table 5 shows the variation of aquifer resistivity and thickness due to lithologic composition, from which the hydraulic conductivity and transmissivity were computed. The calculated hydraulic conductivity ranges from 0.205-3.027 m/day. The highest value was calculated from VES 6 (western part of the study area) and lowest from VES 12 (North eastern part of the study area). Figure 10 shows the contour map of the hydraulic conductivity calculated from VES data. From the contour map it was observed that the western part of the study area has the high values than other parts of the study area. Figure 11 shows 3D map of the groundwater flow direction in the study area. It is observed from the groundwater flow direction map that the groundwater flows towards the western part of the study and this confirmed the reason for high hydraulic conductivity in that area.

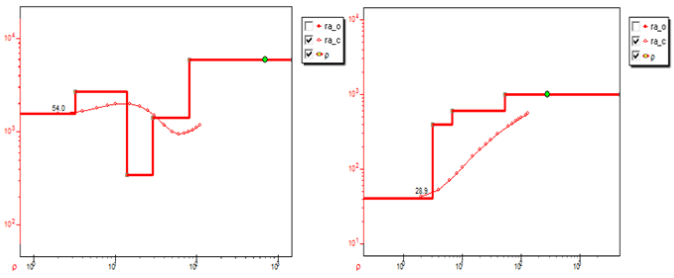

Figure 6e) Curve for VES 9 and 10.

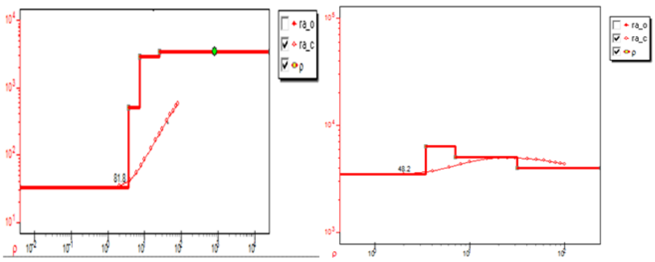

Figure 6f) Curve for VES 11 and 12.

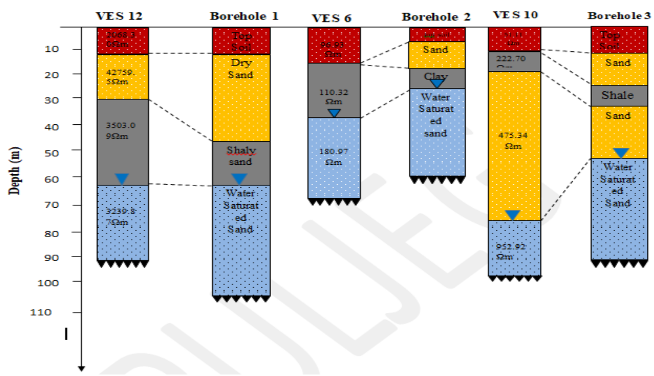

Figure 7) Correlation of geo-electric logs and borehole log of the study area.

HYDROGEOCHEMICAL ANALYSIS RESULTS AND INTERPRETATION

General characteristics of groundwater parameters for the study area revealed that all the 20 samples showed EC values ranged from 10.8 μs/cm to 60.90 μs/cm with a mean value of 30.315 ± 15.166 μs/cm. The

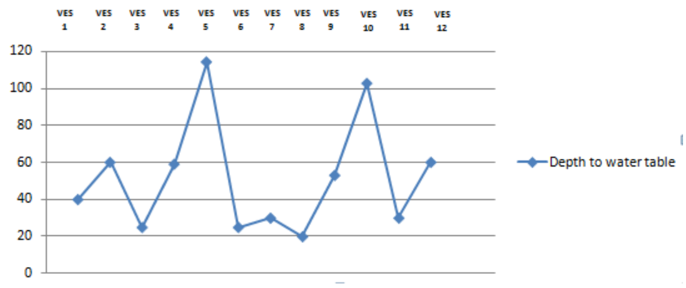

Figure 8) Variations of depth to groundwater.

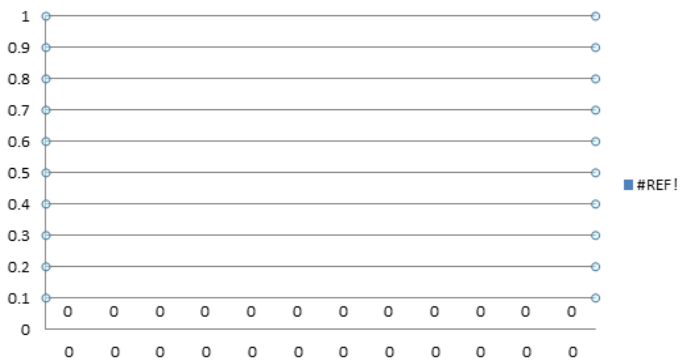

Figure 9) Variations of aquifer thickness in the study area.

TABLE 5
The calculated aquifer parameters from VES

S/N	Latitude	Longitude	Elevation (m)	Depth to water table	Hydraulic head	Aquifer resistivity	Aquifer thickness	Hydraulic conductivity (m/day)	Transmissivity (m²/day)
1	6°12'25.3"	6°49'23.8"	99	40	59	182.86	30	2.998	89.94
2	6°11'13.2"	6°50'18.5"	120	60	60	269.52	40	2.087	83.48
3	6°10'15.8"	6°47'38.2"	48	25	23	954.41	35	0.642	22.47
4	6°09'44.1"	6°46'58.5"	75	59	16	874.16	40	0.697	27.88
5	6°08'07"	6°49'05"	153	114	39	310.83	20	1.828	36.56
6	6°07'07"	6°47'37.1"	30	25	5	180.97	55	3.027	166.49
7	6°12'20.1"	6°52'35.3"	165	30	135	840.82	50	0.722	36.1
8	6°07'9"	6°47'21.1"	48	20	28	226.21	60	2.459	147.54
9	6°12'18.2"	6°50'08.1"	108	53	55	889.53	40	0.685	27.4
10	6°07'33.4"	6°49'12.5"	147	102.5	44.5	952.92	34	0.643	21.862
11	6°10'29.3"	6°47'40.3"	52	30	22	1410.99	50	0.446	22.3
12	6°11'52.2"	6°53'05.7"	146	60	86	3239.87	40	0.205	8.2

concentration of heavy metals such as Fe, Ni, Cd, Cu, Zn, Cr, As, V were found to range from 0 ppm to 3.7690 ppm, 0 ppm to 0.750 ppm, 0.01 ppm to 0.860 ppm, 0 ppm to 0.1050 ppm, 0 ppm to 1.7980 ppm, 0.0022 ppm to 0.0460 ppm, 0 ppm to 0.560 ppm, 0 ppm to 0.008 ppm respectively. The mean concentration of the heavy metals analysed followed

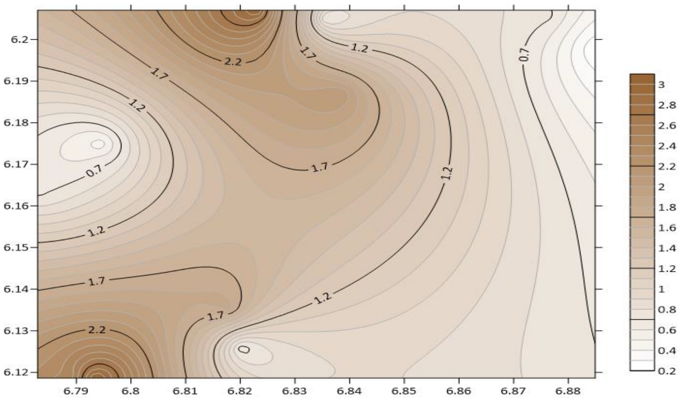

Figure 10) Contour map of hydraulic conductivity calculated from VES data.

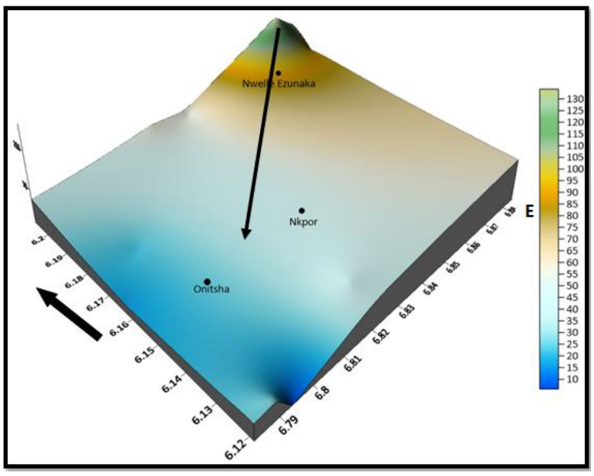

Figure 11) 3D map showing the groundwater flow direction in the study area.

the descending order: Fe>Zn>Cd>Cu>Cr>As>Ni>V. Moreover, the mean value of Fe (0.832000 ± 1.0626228 ppm) and Cd (0.043750 ± 0.0181713 ppm) exceeded the permissible limit for NSDWQ water quality standard. Among the physical parameters, the concentrations of Total Dissolved Solids (TDS) and Total hardness ranged from 20 mg/l to 410 mg/l, and 4 mg/l to 1000 mg/l respectively with mean values of 122 ± 114.78126 mg/l and 65.30 ± 222.35512 mg/l respectively. The high values of standard deviation and variance of the total hardness (222.35512 mg/l and 49441.800 mg/l) respectively shows a wide degree in the variability of groundwater hardness in the area. The pH values of all the samples analysed in the study area ranges from 4.93 to 6.94 with a mean value of 5.6695 ± 0.57242, indicating that the groundwater in the study area is slightly acidic in nature.

However, the mean values of the major Cations and Anions analyzed in this study are below permissible limits of WHO [45] and NSDWQ standards. The cations (Ca, Mg, Na and K) have mean values of 5.4550 ± 3.39077 ppm, 8.3485 ± 5.51415 ppm, 33.0200 ± 18.40748 ppm, and 9.1920 ± 4.47851 ppm respectively while the Anions (Cl^-, SO_4, CO_3 and HCO_3) have mean values of 92.8250 ± 53.82560 ppm, 6.5585 ± 2.94490 ppm, 20.2800 ± 8.28509 ppm and 14.1300 ± 5.95669 ppm respectively. There is a wide degree in the variability of Chloride in the groundwater of the study area; this is evident in the high values of its standard deviation and variance (53.82560 and 2897.196 respectively).

EVALUATION OF DRINKING WATER QUALITY

The Water Quality Index (WQI) is a mathematical techniques used to transform large quantities of water quality data into a single number which represents the water quality level. In this study, the WHO Standard and NSDWQ Standards were used to determine the suitability of the ground water quality for drinking purposes. Table 6 shows the results of the drinking water quality evaluation. Figures 12a-12d shows the bar chart of the HEI, Cd, HPI and WQI respectively.

The characteristics of the groundwater indices evaluation of the study is summarized below (Table 7) with minimum, maximum, mean, and standard deviation values. The study revealed that HEI ranged from 8.85 to 30.70 with mean value of 19.3975 ± 6.78653. The HEI values indicate that 5% and 40% of the samples exhibited low and medium contamination which falls below the means. Based on the HEI values, 55% of the samples showed high contamination. The C_d values ranged from 0.85 to 22.70 with mean value of 11.5976 ± 6.88701. The C_d values have suggested that only 15% of the samples locations are highly polluted in the study area. HPI values showed the mean of 15.6800 ± 16.30768 while the values ranged from 2.69 to 54.96. The WQI ranged from 2.59 to 143.40 with means value of 22.80 ± 33.0140.

TABLE 6
Classification of the groundwater quality of the study area based on modified categories of drinking water quality indices values

Index method	Category	Degree of pollution/ Water class	Number of locations	% of sample	Samples
HEI	<10	Low	1	5	W16
	10-20	Medium	8	40	W2, W3, W4, W5, W11, W14, W15, W18
	>20	High	11	55	W1, W6, W7, W8, W9, W10, W12, W13, W17, W19, W20
C_d	<10	Low	9	45	W2, W3, W4, W5, W11, W14, W15, W16, W18
	10-20	Medium	8	40	W6, W7, W8, W9, W10, W12, W17, W19
	>20	High	3	15	W1, W13, W20
HPI	<10	Low	17	85	W2, W3, W4, W5, W6, W7, W8, W11, W12, W13, W14, W15, W16, W17, W18, W19, W20
	10-20	Medium	3	15	W1, W9, W10
	>20	High	0	0	
WQI	0-25	Excellent	15	75	W2, W3, W4, W5, W6, W7, W8, W11, W13, W14, W15, W16, W17, W18, W19
	>25-50	Good	1	5	W12
	>50-75	Fair	3	15	W9, W10, W20
	>75-100	Poor	0	0	
	> 100-150	Very poor	1	5	W1
	>150	Unfit for drinking	0	0	

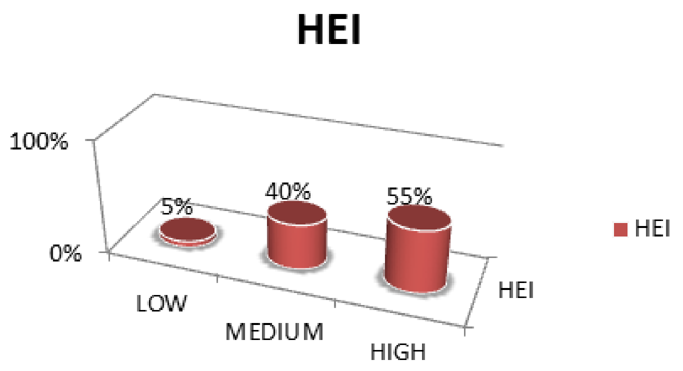

Figure 12a) Heavy Metals Evaluation Index (HEI) of the studied samples.

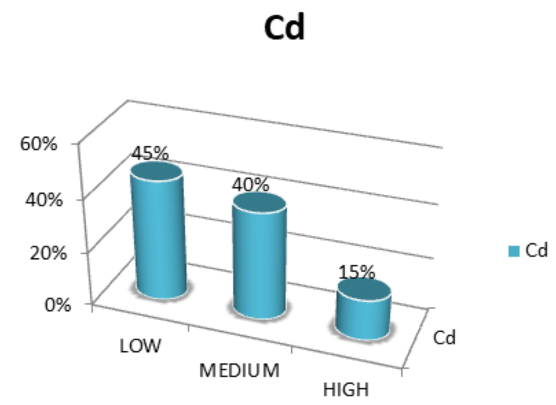

Figure 12b) Degree of contamination (Cd) of the studied samples.

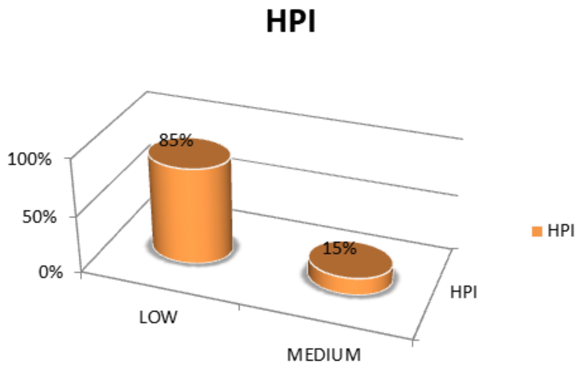

Figure 12c) Heavy Metals Pollution Index (HPI) of the studied samples.

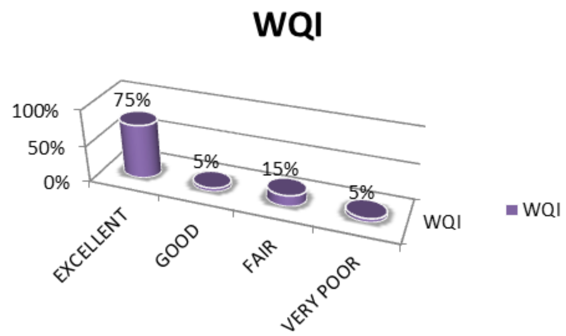

Figure 12d) Water Quality Index (WQI) of the studied samples.

TABLE 7
Descriptive statistics of the groundwater indices evaluation

	N	Range	Minimum	Maximum	Sum	Mean	Std. Deviation	Variance
Heavy metal evaluation index	20	21.85	8.85	30.7	387.95	19.3975	6.78653	46.057
Degree of contamination	20	21.85	0.85	22.7	231.95	11.5976	6.88701	47.431
Heavy metal pollution index	20	52.27	2.69	54.96	313.6	15.68	16.30768	265.941
Water quality index	20	140.81	2.59	143.4	456	22.8	33.0114	1089.753
Valid N (list wise)	20							

TABLE 8
Results interpretation of the various irrigation groundwater quality models for the study area

Index method	Category	Water class	Number of locations	% of sample	Samples
SAR	<10	Excellent	8	40	W2, W4, W9, W13, W14, W17, W19, W20
	10-18	Good	9	45	W1, W3, W6, W7, W8, W10, W11, W16, W18
	18-26	Fair	2	10	W12, W15
	>26	Poor	1	5	W5
KR	<1	Suitable	0	0	Nil
	>1	Unsuitable	20	100	W1, W2, W3, W4, W5, W6, W7, W8, W9, W10, W11, W12, W13, W14, W15, W16, W17, W18, W19, W20
MAR	<50	Acceptable	6	30	W2, W5, W13 W14, W15, W16
	>50	Non-acceptable	14	70	W1, W3, W4, W6, W7, W8, W9, W10, W11, W12, W17, W18, W19, W20
Na %	<20	Excellent	0	0	Nil
	20-40	Good	1	5	W14
	40-60	Permissible	11	55	W2, W3, W4, W9, W10, W11, W13, W17, W18, W19, W20
	60-80	Doubtful	8	40	W1, W5, W6, W7, W8, W12, W15, W16
	>80	Unsuitable	0	0	Nil
PI	>75	Excellent	14	70	W1, W2, W5, W6, W7, W8, W9, W10, W12, W13, W14, W15, W16, W20
	25-75	Good	6	30	W3, W4, W11, W17, W18, W19
	<25	Unsuitable	0	0	Nil

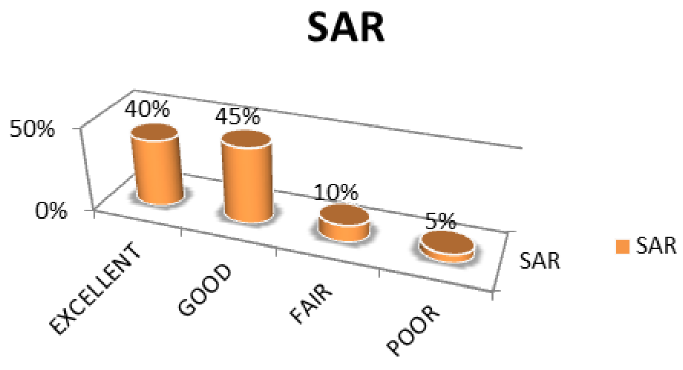

Figure 13a) Sodium Adsorption Ratio (SAR) of the studied samples.

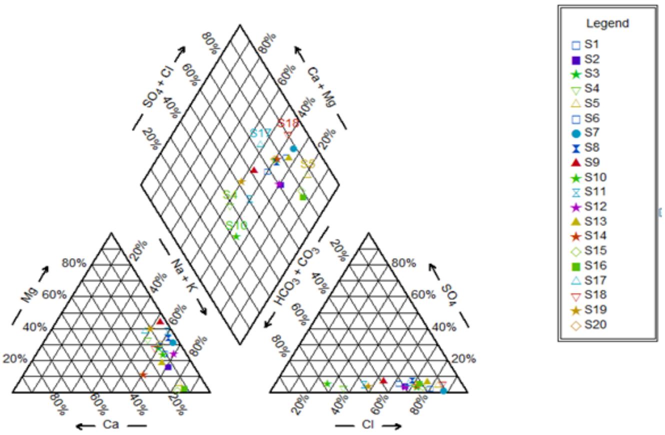

Figure 14) Piper diagram of the studied samples.

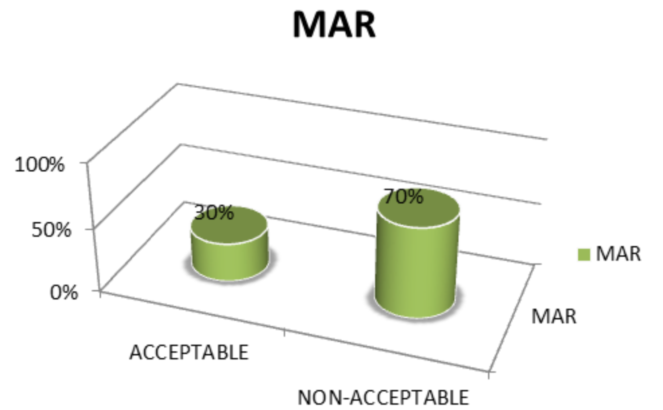

Figure 13b) Magnesium Adsorption Ratio (MAR) of the studied samples.

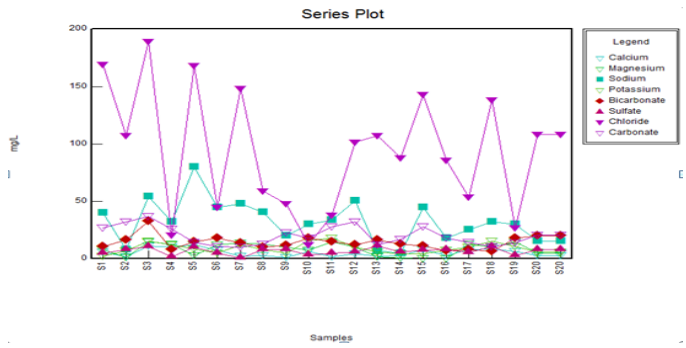

Figure 15) Series plot of the groundwater in the study area.

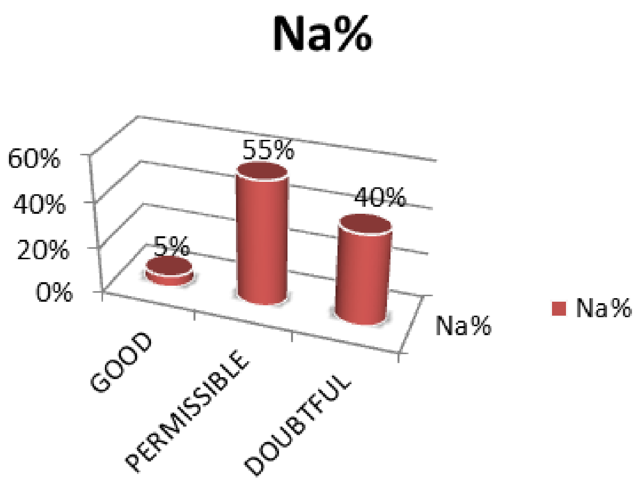

Figure 13c) Sodium percentage (Na%) of the studied samples.

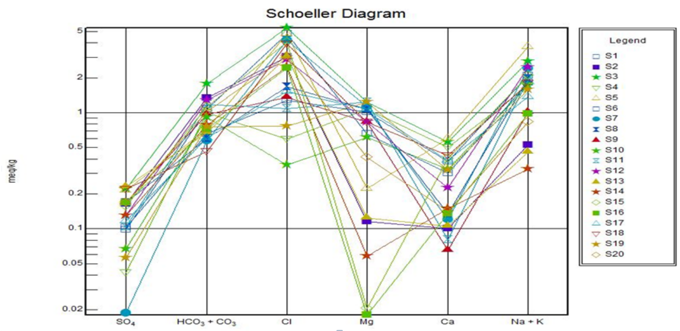

Figure16) Schoeller diagram of the groundwater in the study area.

groups of water types and it was used to determine the hydrochemical facies of the groundwater in the study area (Figure 14). The diagram revealed that groundwater facies of the study area are dominantly sodium chloride water type.

Series plot

This is one of the hydrochemical facies classification used in this study. It gives an instantaneous picture of the dominant facies in the groundwater. The series plot of this study is shown in Figure 15 below and it shows that the dominant parameters are the chloride and sodium thus Sodium Chloride water type. The series plot agrees with the piper diagram.

Schoeller diagram

This diagram allows us to make a visual comparison of the composition of different water samples. They are plotted on six equally spaced logarithmic scales in the arrangement. It was proposed by [46] to plot the concentration of anions and cations. The Schoeller diagram of this study is shown in Figure 16 below and it indicates that the groundwater in the study area is dominantly sodium chloride type [30]. This is in the agreement with other hydrochemical facies classification models applied in this study.

CONCLUSION

The use of electrical resistivity and hydrochemical analysis helps reduce the additional expenditures of carrying out pumping tests and offer an alternative approach for estimating the hydraulic parameters, as it would give pre-drilling estimation of the yield of a prospective borehole in the area. The study area is drained by three major rivers (Anambra, Idemmili and Nkisi) each flowing west ward into the river Niger. Mean annual rainfall is about 2042.65 mm. The result of the VES survey revealed that the subsurface layers ranged from 3 to 6 but dominated by 4 layers and litho-logs from boreholes confirmed it. The depth to water ranges from 25 m to 114 m. Aquifer thicknesses range between 20 m to and 60 m. The hydraulic conductivity (K) ranged from 0.25 m/day to 3.027 m/day while the transmissivity (T) ranged from 8.2 m^2/day to 166.49 m^2/day. Hydrochemical analysis of ground water samples from the study area reveals that all ionic components are within the acceptable limits, with the exception of heavy metals like Fe and Cd. The pH values reveal that they are acidic waters. Based on the WQI; 80% of the samples belongs to excellent to good water quality type, whereas 20% belongs to fair to very poor water quality for drinking purposes in the study area. In the pollution evaluation indices classification; HEI, Cd and HPI showed that 5%, 45% and

85% of the samples reveals low level of pollution in the area respectively. For the assessment of water quality for irrigation purposes, Sodium Adsorption Ratio (SAR) model revealed that 40% (8 samples) of the samples were excellent for irrigation, 45% (9 samples) are of good quality, 10% (2 samples) were fair while 5% (1 sample) is of poor quality for irrigation. However, Kelly's Ratio (KR) model shows that 100% of the samples are unsuitable for irrigation purposes while the Magnesium Adsorption Ratio (MAR) revealed that 30% (6 samples) of the samples are acceptable and 70% (14 samples) not acceptable. Moreover, the Sodium Percentage (Na%) model revealed that only 5% (1 sample) of the samples is good for irrigation, 55% (11 samples) are permissible while 40% (8 samples) are doubtful. The Permeability Index (PI) revealed that 70% of the samples are of excellent quality while 30% are of good quality for irrigation purposes. Classification of the hydrochemical facies using Piper diagram, Stiff diagram and series plots confirms that the ground waters in the study area are dominantly sodium chloride waters.

It is hoped that this study will serve as a source of background information for physicochemical parameters, water quality indices, as well as database for spatial distribution of heavy metal and other quality parameters. This study is expected to help water resource planners taking adaptive measures for groundwater quality monitoring in the study area.

REFERENCES

1. Olaswhinde PI, Amadi AN, Idris NA, et al. Aquifers Characterization in Agaie, North-Central Nigeria Using Electrical Resistivity Method and Borehole Lithologs. Am. J. Environ. Prot. 2015; 3(3), 60-66.
2. UNESCO. Water: A shared responsibility. The United Nations World Water Development. 2, Barcelona, 2006.
3. Adeniji AE, Ajala A, Osho JK. Estimation of groundwater potential using surficial resistivity measurements: A case study from parts of Makurdi benue state, Nigeria. Global J Pure Appl Sci. 2017; 23(2): 311-320.
4. Al Sabahi E, Rahim SA, Wan Zahairi WY et al, Nozaily AI et al, Alshaebi F et al. The characteristics of leachate and groundwater pollution at municipal solid waste landfill of Ibb City, Yemen. Am J Environ Sci. 2009; 5(3):256-266.
5. Reyment RA. Aspects of the Geology of Nigeria, University of Ibadan press. 1965;42-115.
6. Zhang J, Zhou Y, Li R, et al. Accuracy Assessments and Uncertainty Analysis of Spatially Explicit Modeling for Land Use/Cover Change and Urbanization: A case in Beijing Metropolitan Area. China Earth Sci. 2010; 53(2): 173-180.
7. Singh KK, Singh KA, Singh K B. 2D resistivity imaging survey for sitting water supply tube wells in metamorphic terrains: A case study of CMRI campus, Dhanbad, India. The Leading Edge. 2006; 25(12):1458.
8. Batte, AG, Muwanga, A et al, Sigrist et al, WP et al. Evaluating the Use of Vertical Electrical Sounding as a Groundwater Exploration Technique to Improve on the Certainty of Borehole Yield in Kamuli District (Eastern Uganda). African J. Sci. Technol. 2008; 9: 72-85.
9. Hubbard, SS, Peterson, JE et al, Majer JR et al, Zawislanski et al, E. L et al, Williams et al, PT et al, Robert et al, K.H et al, Wobber F et al. Estimation of permeable Pathways and Water Content using Tomographic Radar data. Leading Edge. 1997; 16 (11): 1623-1628.
10. Vereecken H, Binley A, Cassiani G, at el. Applied Hydrogeophysics, The series is published by ISO Press, Amsterdam and Springer in Conjunction with the NATO, Public Diplomacy Divition. 2006; 376.
11. Aizebeokhai AP, Oyebanjoet OA, et al. Application of vertical electrical soundings to characterize aquifer potential in Ota, Southwestern, Nigeria. International Journal of Physical Sciences, 2013; 46(8): 2077-2085.
12. Iduma REO, Abam TKS, Uko ED, et al. Dar Zarrouk Parameter as a Tool for Evaluation of Well Locations in Afikpo and Ohaozara, Southeastern Nigeria. J Water Resource Prot. 2016; 8(4): 505-521.
13. Todd, K D, Mays, LW, et al. Groundwater Hydrology. 3rd ed. John Wiley and Sons. New York, 2005:636.
14. Yadav GS, Abolfazli H. Geoelectrical soundings and their relationship to hydraulic parameters in semi-arid regions of Jalore, Northwestern India. J Appl Geophys. 1998; 39(1):35-51.
15. Urish DW. Electrical resistivity-hydraulic conductivity relationships in glacial outwash aquifers. Water Resour Res.1981; 17(5):1401-1408.
16. Laouini G, Etuk SE, Agbasi OE (2017). Delineation of Aquifers Using Dar Zarrouk Parameters in Parts of Akwa Ibom, Niger Delta, Nigeria. J Hydrogeol Hydrol Eng. 2017; 6(1).
17. Kelly WE. Geoelectric sounding for estimating aquifer hydraulic conductivity. Ground Water. 1977; 15(6): 420-425.
18. Heigold PC, Gilkeson RH, Cartwright K et al, Reid PC et al. Aquifer transmissivity from surficial electrical methods. Ground Water. 1979; 17(4): 330-345.
19. Niwas S, Singhal DC. Estimation of aquifer Transmissivity from Dar-Zarrouk parameters in porous media. J. of Hydrology. 1981; 50:393-399.
20. Kosinki WK, Kelly WE. Geoelectric sounding for predicting aquifer properties. Ground Water. 1981; 19 (2): 163-171.
21. Schimschal U. The relationship of geophysical measurements to hydraulic conductivity at the Brantley dam site, New Mexico. Geoexploration. 1981; 19(2): 115-125.
22. Mazac O, Kelly WE Landa I. A hydrogeophysical model for relations between electrical and hydraulic properties of aquifers. J. Hydrol. 1985; 79:1-19.
23. Huntley D. Relations between permeability and electrical resistivity in granular aquifers. Ground Water. 1986; 24(4): 466-474.
24. Frolich RK, Kelly WE. Estimates of specific yield with the geoelectrical resistivity method in glacial aquifers. J. Hydrology.1988; 97(1-2): 33-44.
25. Kenneth S. Okiongbo, Edirin, et al. Determination of Aquifer Properties and Groundwater Vulnerability Mapping Using Geoelectric Method in Yenagoa City and Its Environs in Bayelsa State, South South Nigeria. 2012; 4(6):17-30.
26. Mbonu DDC, Ebeniro JO, Ofoegbu CO et al, Ekine AS et al. Geoelectrical sounding for the determination of aquifer characteristics in parts of the Umuahia area of Nigeria. Geophysics. 1991; 56(5):284-291.
27. Kalinski KJ, Kelly WE, Bogardi I. Combined use of geoelectric sounding and profiling to quantify aquifer protection properties. Ground Water. 1993; 31(4): 538-544.
28. Frolich RK, Urish D. The use of geoelectrics and test wells for the assessment of groundwater quality of a coastal industrial site. J. Applied Geophysics. 2002;50(3): 261-278.
29. Lashkaripour GR. An investigation of groundwater condition by geoelectrical resistivity method: A case study in Krin aquifer southeast Iran. J. Spatial Hydrology. 2003; 3(1): 1-5.
30. Louis IF, Karantonis GA, Voulgaris NS et al, Louis FI et al. The contribution of geophysical methods in the determination of aquifer parameters: The case of Mornos River Delta, Greece. J Chem En Sci. 2005; 8(4): 41-49.
31. Singh K.P. Nonlinear estimation of aquifer parameters from surficial resistivity measurements. Hydrol. Earth Sys. Sci. Discuss. 2005; 2: 917-938.
32. Agbasi, O.E, Etuk et al, S.E et al. Hydro-Geoelectric Study of Aquifer Potential in Parts of Ikot Abasi Local Government Area, Akwa Ibom State, Using Electrical Resistivity Soundings. Int. J. Geol. Earth Sci. 2016; 2(4): 43-54.
33. Johnson, HK. A man/computer interpretation system for resistivity soundings over a horizontally stratified earth. Geophysical Prospecting. 1977; 25(4):667-691.
34. Kenneth S. Okiongbo, Edirin, et al. Determination of Aquifer Properties and Groundwater Vulnerability Mapping Using Geoelectric Method in Yenagoa City and Its Environs in Bayelsa State, South South Nigeria. 2012; 4(6):17-30.
35. Worthington PF. The uses and abuses of the Archie equations: the formation—porosity relationship. J Appl Geophys. 1993; 30(3): 215-228.
36. Garnier, B. J. Weather condition in Nigeria. Climatological Research Series, No. 2 McGrill University, Montreal, Canada. 1967.
37. Asowata TI, Olatunji AS. Enrichmentof trace elements in urban

soils and sediments in a typical sedimentary environments; Onitsha metropolis southeastern Nigeria. Environ Geol. 2018; 2(2): 47-60.

38. Ofulume AB, Ibeneme IS, Orazulike DM, et al. The Gboko Limestone, Yandev, Benue State, Nigeria: Geology, Geochemistry and Industrial Potentials. 2017; 7(2).

39. Nwajide, C. S. Nigeria Sedimentary Basins. 2013; 321-332.

40. Bhattacharya PK, Patra HP. Direct current geoelectric sounding: principles and interpretation. Elsevier Science Publishing Co., Inc., Amsterdam. 1st Edition. 1968.

41. Chakravarthi V, Shankar GBK, Muralidharan D et al, Harinarayana T et al, Sundararajan N et al. An integrated geophysical approach for imaging subbasalt sedimentary basins: case study of Jam River Basin, India. Geophysics. 2007; 72(6):141-147.

42. Todd D.K Groundwater Hydrology second edition. Wiley, New York, 1980:552.

43. Zohdy AAR, Eaton GP, Mabey DR. Application of surface geophysics to groundwater investigations. United State Geophysical Survey, Washington, 1974.

44. Washington D.C. Standard Methods for the Examination of Water and Waste Water. APHA (America Public Health Association), 1985: 4-17.

45. World Health Organization WHO: Guidelines for drinking water quality criteria, 4th ed. Geneva, 2011:307-441.

46. Schoeller, H. Groundwater. Dynamic and chemical hydrology, Research, Exploitation and Assessment of Resources. Internationale Revue der gesamten Hydrobiologie und Hydrographie. 1962; 49(1):182.